Chapter 29

$D^0 - \overline{D}^0$ Mixing[1]

Meson-antimeson oscillations have been of central importance in the evolution of the Standard Model (SM) and in searches for New Physics. This is based on two seminal features [1]: (a) In such oscillations quantum mechanical effects will build up over macroscopic distances, which makes tiny mass differences measurable. (b) Oscillations and the rare decay reactions $s \to dl^+l^-$, $s \to d\nu\overline{\nu}$, $b \to s\gamma$, and $b \to sl^+l^-$ are driven by flavor changing neutral currents (FCNC), which are highly suppressed in the SM, where they are given by 1-loop processes.

Short-distance dynamics in the form of the well-known quark-box diagrams provide a good approximation for the effective $\Delta B = 2$ and the **CP** violating $\Delta S = 2$ transition operators with the superheavy top mass providing a moderate enhancement rather than the considerable GIM suppression inherent in m_c^2/M_W^2 etc.; it provides a significant contribution even for ΔM_K. The situation is fundamentally different for neutral mesons built from the *up*-type quarks (u, c, t) for a number of reasons: (i) Since top quarks decay before they can hadronize, there are no T^0 mesons, and $T^0 - \bar{T}^0$ oscillations a forteriori cannot occur. (ii) Neither can pion etc. oscillations, since pion and eta mesons are their own antimesons. (iii) Oscillations can thus proceed only for neutral D mesons, which makes charm quite unique among up-type quarks.

While $D^0 - \bar{D}^0$ oscillations do have to proceed on some level, we know on general grounds that they have to be rather slow in the SM. For while the amplitude for $D^0 \Rightarrow \bar{D}^0$ is doubly Cabibbo suppressed, its leading decay channels are not. Furthermore $D^0 - \bar{D}^0$ oscillations have to vanish already in the $SU(3)_{Fl}$ symmetry limit, which represents a considerably better approximation to the real world than the $SU(4)_{Fl}$ or $SU(6)_{Fl}$ symmetry limits constraining $K^0 - \bar{K}^0$ and $B^0 - \bar{B}^0$ oscillations, respectively. As discussed below within the SM $D^0 - \bar{D}^0$ oscillations are driven by long distance dynamics, over which our theoretical control is rather limited. It is quite difficult to make the statement that these oscillations are slow more specific. Nevertheless it is mandatory to probe $D^0 - \bar{D}^0$ oscillations as sensitively as possible; while their observation by themselves might not provide conclusive proof for the intervention of New Physics, it is an essential element in searches for CP violation, where such conclusive proof can be obtained.

[1]By David Asner and Haibo Li

29.1 Theoretical Review

29.1.1 Oscillation Formalism: the Phenomenology

It has become customary to use the terms 'oscillations' and 'mixing' in an interchangeable way. This is unfortunate. For while the two terms describe phenomena that are related, they are of a different nature with 'mixing' denoting the more general concept and 'oscillations' the more specific one.

Mixing means that classically distinct states are not necessarily so in quantum mechanics and therefore can *interfere*. For example in atomic physics wave functions are said to be *mixtures* of 'right' and 'wrong' components whose interference generates parity odd observables; it is the weak neutral current that induces such wrong parity component. Or mass eigenstates of quarks (and leptons) contain components of different flavors giving rise to a non-diagonal CKM (or PMNS) matrix described later. This is usually referred to as quark mixing. Such mixing creates a plethora of observable effects.

The most intriguing ones arise when the violation of a certain quantum number – like strangeness – leads to the stationary or mass eigenstates not being eigenstates under that quantum number. This induces *oscillations* like matter-antimatter oscillations discussed above or neutron-antineutron oscillations or neutrino oscillations. *Oscillations* thus require *mixing*, but go beyond it in the sense that they generate transitions with a very peculiar time evolution, namely an oscillatory one rather than the usual exponentially damped one.

The time evolution of the $D^0 - \overline{D}^0$ system is described by the Schrödinger equation as

$$i\frac{\partial}{\partial t}\begin{pmatrix} D^0(t) \\ \bar{D}^0(t) \end{pmatrix} = \left(\mathbf{M} - \frac{i}{2}\mathbf{\Gamma}\right)\begin{pmatrix} D^0(t) \\ \bar{D}^0(t) \end{pmatrix}, \tag{29.1}$$

where the $\mathbf{M}$ and $\mathbf{\Gamma}$ matrices are Hermitian, and are defined as

$$\left(\mathbf{M} - \frac{i}{2}\mathbf{\Gamma}\right) = \begin{pmatrix} M_{11} - \frac{i}{2}\Gamma_{11} & M_{12} - \frac{i}{2}\Gamma_{12} \\ M_{12}^* - \frac{i}{2}\Gamma_{12}^* & M_{22} - \frac{i}{2}\Gamma_{22} \end{pmatrix}. \tag{29.2}$$

CPT invariance imposes

$$M_{11} = M_{22} \equiv M\,,\ \Gamma_{11} = \Gamma 22 \equiv \Gamma. \tag{29.3}$$

The off-diagonal elements of these matrices describe the dispersive and absorptive parts of $D^0 - \overline{D}^0$ mixing (for details see [227]). The two eigenstates D_1 and D_2 of the effective Hamiltonian matrix $(\mathbf{M} - \frac{i}{2}\mathbf{\Gamma})$ are given by

$$|D_1\rangle = \frac{1}{\sqrt{|p|^2 + |q|^2}}(p|D^0\rangle + q|\overline{D}^0\rangle)\,,\ |D_2\rangle = \frac{1}{\sqrt{|p|^2 + |q|^2}}(p|D^0\rangle - q|\overline{D}^0\rangle). \tag{29.4}$$

The corresponding eigenvalues are

$$\lambda_{D_1} \equiv m_1 - \frac{i}{2}\Gamma_1 = \left(M - \frac{i}{2}\Gamma\right) + \frac{q}{p}\left(M_{12} - \frac{i}{2}\Gamma_{12}\right), \tag{29.5}$$

$$\lambda_{D_2} \equiv m_2 - \frac{i}{2}\Gamma_2 = \left(M - \frac{i}{2}\Gamma\right) - \frac{q}{p}\left(M_{12} - \frac{i}{2}\Gamma_{12}\right), \tag{29.6}$$

where $m_1(m_2)$ and $\Gamma_1(\Gamma_2)$ are the mass and width of D_1 (D_2), respectively, and

$$\left|\frac{q}{p}\right|^2 = \frac{M_{12}^* - \frac{i}{2}\Gamma_{12}^*}{M_{12} - \frac{i}{2}\Gamma_{12}}. \tag{29.7}$$

¿From Eqs.(29.5) and (29.6), one can get the differences in mass and width:

$$\Delta m \equiv m_2 - m_1 = -2Re\left[\frac{q}{p}(M_{12} - \frac{i}{2}\Gamma_{12})\right], \tag{29.8}$$

$$\Delta\Gamma \equiv \Gamma_1 - \Gamma_2 = -2Im\left[\frac{q}{p}(M_{12} - \frac{i}{2}\Gamma_{12})\right]. \tag{29.9}$$

The subscripts and are mere labels at this point. We have chosen the definitions of ΔM and $\Delta\Gamma$ s.t. when applied to the kaon sector with $K_S = K_1$ and $K_L = K_2$, we get both differences positive.

A pure D^0 state generated at $t = 0$ could decay to $K^+\pi^-$ state either by $D^0 - \overline{D}^0$ mixing or by DCSD, and the two amplitudes may interfere. The time evolutions of $|D_1\rangle$ and $D_2\rangle$ are given by

$$|D_i\rangle = e_i|D_i\rangle\,,\ e_i = e^{-im_i t - \frac{1}{2}\Gamma_i t}\,,\ (i = 1, 2). \tag{29.10}$$

Under the phase convention $CP|D^0\rangle = |\overline{D}^0\rangle$, a state that is purely $|D^0\rangle$ ($|\overline{D}^0\rangle$) prepared by the strong interaction at $t = 0$ will evolve to $|D^0_{phys}(t)\rangle$ ($|\overline{D}^0_{phys}(t)\rangle$):

$$|D^0_{phys}(t)\rangle = g_+(t)|D^0\rangle + \frac{q}{p}g_-(t)|\overline{D}^0\rangle\,, \tag{29.11}$$

$$|\overline{D}^0_{phys}(t)\rangle = \frac{p}{q}g_-(t)|D^0\rangle + g_+(t)|\overline{D}^0\rangle\,, \tag{29.12}$$

where

$$g_\pm(t) = \frac{1}{2}(e_1 \pm e_2). \tag{29.13}$$

The probability to find a $\overline{D}^0$ at time t in an initially pure D^0 beam is given by

$$|\langle\overline{D}^0|D^0_{phys}(t)\rangle = \frac{1}{4}\left|\frac{q}{p}\right|^2 e^{-\Gamma_2 t}\left(1 + e^{-\Delta\Gamma t} - 2e^{-\frac{1}{2}\Delta\Gamma t}cos\Delta m t\right). \tag{29.14}$$

While the flavour of the initial meson is tagged by its production, the flavour of the final meson is inferred from its decay.

There are two dimensionless ratios describing the interplay between oscillations and decays:

$$x \equiv \frac{\Delta m}{\Gamma}\,,\ y \equiv \frac{\Delta\Gamma}{2\Gamma}, \tag{29.15}$$

where $\Gamma \equiv (\Gamma_1 + \Gamma_2)/2$ is the averaged D^0 width.

29.1.2 Standard Model Predictions for Oscillation Parameters

Oscillations arise from $\Delta C = 2$ interactions that generate off-diagonal terms in mass matrix as in Eq.(29.2) for D^0 and $\overline{D}^0$ mesons. The expansion of the off-diagonal terms in the neutral D mass matrix to second order in perturbation theory is

$$M_{12} = \langle \overline{D}^0 | \mathcal{H}_w^{\Delta C=2} | D^0 \rangle + P \sum_n \frac{\langle \overline{D}^0 | \mathcal{H}_w^{\Delta C=1} | n \rangle \langle n | \mathcal{H}_w^{\Delta C=1} | D^0 \rangle}{m_D^2 - E_n^2}\,, \tag{29.16}$$

$$\Gamma_{12} = \sum_n \rho_n \langle \overline{D}^0 | \mathcal{H}_w^{\Delta C=1} | n \rangle \langle n | \mathcal{H}_w^{\Delta C=1} | D^0 \rangle\,, \tag{29.17}$$

where the sum runs over all relevant intermediate states (virtual ones for M_{12} and real ones for Γ_{12}), P denotes the principle value, and ρ_n is the density of the states n.

The operator in the first term – $\mathcal{H}_w^{\Delta C=2}$ – is a *local* one at scale $\mu \sim m_D$, so it contributes to the M_{12} (but not to the Γ_{12}) part of the generalized mass matrix. New Physics could induce such a contribution of potentially significant size. The SM generates such a term, namely from the quark box diagram with b quarks as internal quarks, yet it is truly tiny due to its highly suppressed CKM parameters. The second term in Eq. (29.16) comes from a double insertion of $\Delta C = 1$ operators; it contributes to both M_{12} and Γ_{12}. The dominant SM contribution comes from here as described below; New Physics could make here a significant contribution to M_{12}.

BES-III-20050721-1

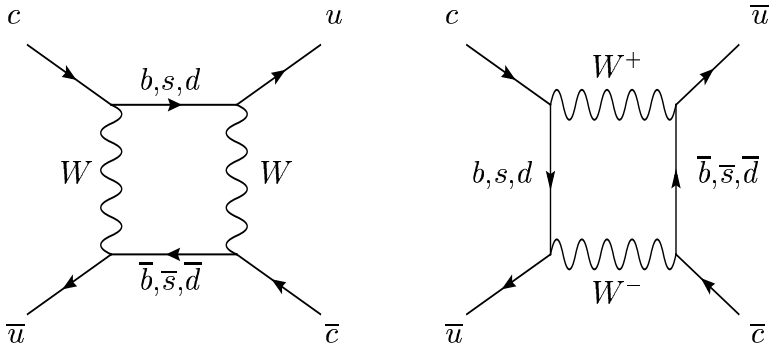

Figure 29.1: Standard Model box diagrams of flavor-changing neutral currents contributing to $D^0 - \overline{D}^0$ mixing at the quark level.

Short-Distance Contribution to x and y

In the SM there is a bona fide short-distance $\Delta C = 2$ operator, which is inferred from the quark box diagram with b quarks as the intermediate quarks, see Fig. 29.1. The effects due to intermediate b quarks are evaluated in a straightforward way since they are far off-shell [228]:

$$\Delta m^{b\bar{b}} \simeq -\frac{G_F^2 m_b^2}{8\pi^2} |V_{cb}^* V_{ub}|^2 \frac{\langle D^0 | (\overline{u}\gamma_\mu(1-\gamma_5)c)(\overline{u}\gamma_\mu(1-\gamma_5)c) | \overline{D}^0 \rangle}{2M_D}\,; \tag{29.18}$$

however they are highly suppressed by the tiny CKM parameters. Using factorization to estimate the matrix element one finds $x^{b\overline{b}} \sim 10^{-6}$. Loops with one b and one light quark likewise are suppressed.

For the light intermediate quarks – d, s – the momentum scale is set by the *external* mass m_c. However, it is highly GIM suppressed

$$\Delta m^{(s,d)} \simeq -\frac{G_F^2 m_c^2}{8\pi^2} |V_{cs}^* V_{us}|^2 \frac{(m_s^2 - m_d^2)^2}{m_c^4} \times \frac{\langle D^0 | (\overline{u}\gamma_\mu(1-\gamma_5)c)(\overline{u}\gamma_\mu(1-\gamma_5)c) + (\overline{u}(1+\gamma_5)c)(\overline{u}(1+\gamma_5)c) | \overline{D}^0 \rangle}{2M_D} . \quad (29.19)$$

In contrast to $K^0 - \overline{K}^0$ and $B^0 - \overline{B}^0$ mixing, the internal quarks in the box diagrams here are down-type quarks. The b-quark contribution, which would give in principle the largest GIM violation, is suppressed by small CKM mixing factors $V_{cb}^* V_{ub}$. The leading contribution, as shown in Eq. (29.19), is given by the strange quark and therefore results in a very effective GIM suppression.

The contribution to $\Delta\Gamma$ from the bare quark box is greatly suppressed by a factor m_s^6. The GIM mass insertions yield a factor m_s^4. Contrary to the claim in Ref. [229] the additional factor of m_s^2 is *not* due to helicity suppression – the GIM factors already take care of that effect; it is of an accidental nature: it arises because the weak currents are purely $V - A$ and only in four dimensions. Including radiative QCD corrections to the box diagram yields contributions $\propto m_s^4 \alpha_S/\pi$. Numerically one finds:

$$y^{box} \ll x^{box} \simeq (10^{-6}) - (10^{-5}). \quad (29.20)$$

Long-distance Contribution to x and y

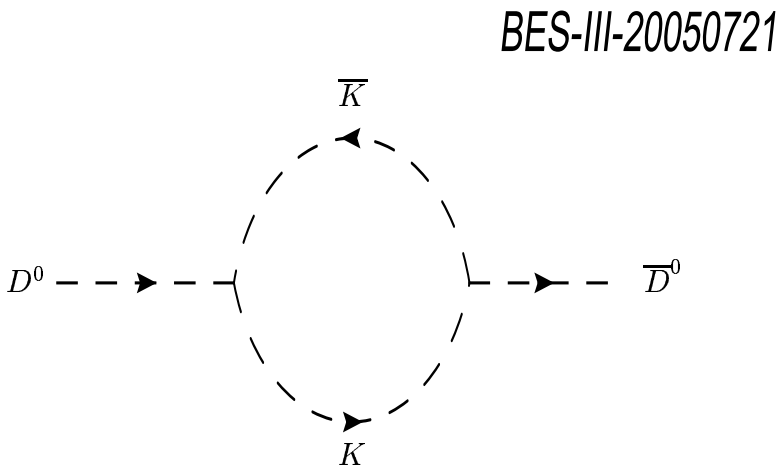

Figure 29.2: A hadron-level diagram of a long-distance physics contribution to $D^0 - \overline{D}^0$ mixing.

The long-distance contributions to $D^0 - \overline{D}^0$ oscillations are inherently non-perturbative, and we have not learnt yet how to calculate them from first principles. It is however ex-

tremely important to estimate their size in order to understand the origin of a possible experimental observation. These contributions come from transitions to final states $|f\rangle$ that are accessible to both $|D^0\rangle$ and $|\overline{D}^0\rangle$. For example, Figure 29.2 illustrates a contribution to mixing from transitions to two pseudoscalars. GIM cancellations are such that they become complete in the $SU(3)_{Fl}$ limit; i.e., no oscillations can occur then.

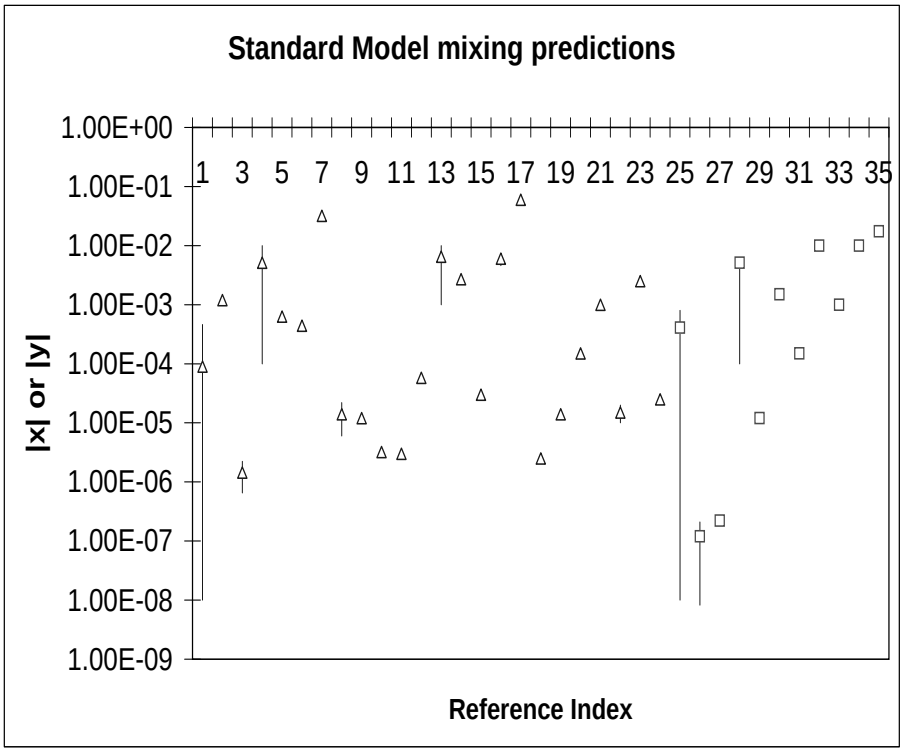

Figure 29.3: Standard Model predictions for $|x|$ (open triangles) and $|y|$ (open squares). Horizontal line references are tabulated in Table **??** in Ref. [230].

Within the SM x and y are generated only at second order in $\mathrm{SU}(3)_F$ breaking,

$$x\,,\,y \sim \sin^2\theta_C \times [SU(3)\text{ breaking}]^2\,, \tag{29.21}$$

where θ_C is the Cabibbo angle. The SM predictions for x and y thus depend crucially on estimating the size of $\mathrm{SU}(3)_F$ breaking. Although y is expected to be determined by SM processes, its value nevertheless affects significantly the sensitivity to new physics of experimental analyses of D mixing [231]. This circumstance would lead to the naive estimate

$$x\,,\,y \sim \sin^2\theta_C \times \left(\frac{m_s}{\Lambda_{hadron}}\right)^2 \leq O(10^{-3}), \tag{29.22}$$

with $\Lambda_{hadron} \sim O(1)$ GeV a typical hadronic scale. Beyond this simple estimate, there are two main approaches to estimating the long-distance contributions to mixing: an *inclusive* approach using an operator product expansion (OPE), and an *exclusive* approach that sums over intermediate hadronic states using experimental data. Neither approach yields accurate predictions.

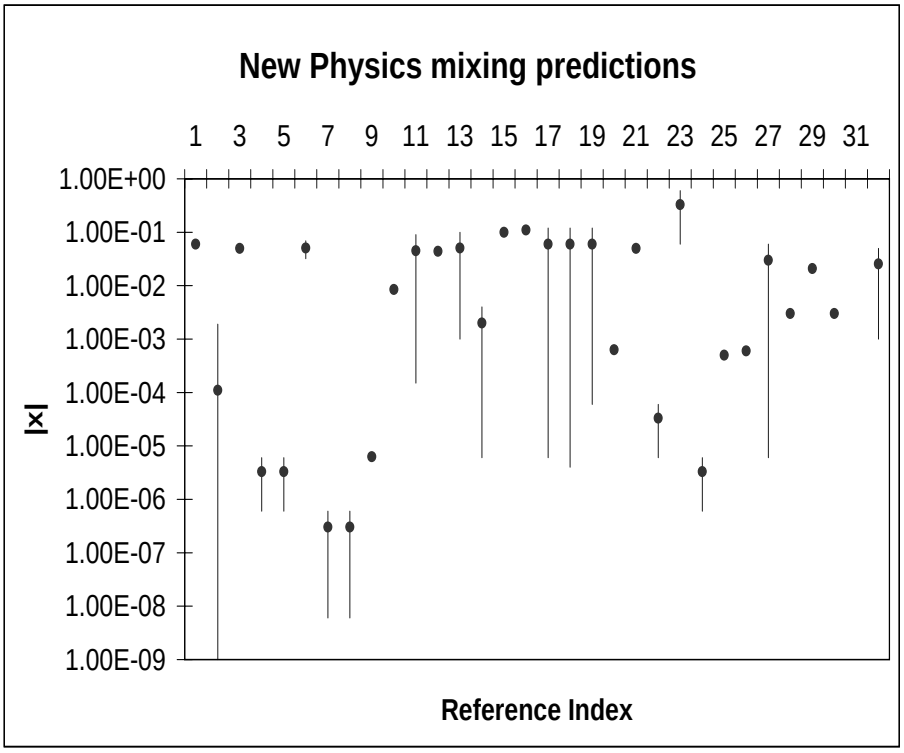

Figure 29.4: New Physics predictions for $|x|$. Horizontal line references are tabulated in Table **??** in Ref. [230].

The *inclusive* approach applies Heavy-Quark Expansions (HQE) to calculate contributions to D oscillations, an approach first taken by H. Georgi [232]and later extended by others [233, 234]. There are two main assumptions. The first is that the mass of the c-quark is large, $m_c \ll \Lambda_{hadr.}$. The second is that one can construct local quark-level operators that can be applied to hadron-level processes, i.e. that quark-hadron duality is applicable already at the charm scale. x and y are evaluated through the OPE as an expansion in powers of $(\Lambda_{hadr.}/m_c)$. The result of this type of approach is [234]

$$x \sim y \sim O(10^{-3}). \tag{29.23}$$

The *exclusive* approach takes all of the known hadronic states common to $|D^0\rangle$ and $|\overline{D}^0\rangle$, and groups them both according to their respective $SU(3)_F$ multiplets and to the number of particles in the final state. An example of such a set would be ($\pi^+\pi^-$, π^+K^-, K^+K^-, $K^+\pi^-$). In the limit of a perfect $SU(3)_F$ symmetry, the individual contributions within each of these groups would cancel, and there would be no mixing. If one knows the relative amplitudes and strong phases for these states, calculations of x and y can be done for each multiplet. For the example set above, this calculation gives a small contribution due to cancellations, a reasonable result since all of the states in the set are far from threshold and not affected as much by phase space considerations. Contributions to x are not required to be on-shell, so in this case there is no symmetry breaking caused by limited phase space. If one assumes that all of the sets contribute incoherently in roughly

the same amount, one concludes that [228]

$$x \leq O(10^{-3}). \tag{29.24}$$

By contrast, contributions to y are due to on-shell states, so phase space is a significant source of symmetry breaking. Considering phase space as the only source of symmetry breaking, one can calculate the contribution to y of each of the final state multiplets for which there is data using the measured masses of the final-particles [230]. The largest calculable contribution comes from the final-state multiplet comprising four pseudoscalars, whose elements are either near the production threshold with relatively large branching fractions, or are above threshold and entirely absent. This ansatz leads to [230]

$$x \leq O(10^{-2}). \tag{29.25}$$

The results from these two methods should not be seen as inconsistent. Rather they indicate the range of uncertainty, which can be phrased as follows: While the best a priori SM estimate yields x, $y \sim O(10^{-3})$, we cannot conclude that values as 'high' as 10^{-2} would necessarily establish the intervention of New Physics. To be more specific: while the presence of New Physics can enhance x to its present upper bound of few $\times 10^{-2}$, it should not affect y in a significant way, since $\Delta\Gamma$ is generated from *on*-shell transitions. The minimal requirement for any claim of New Physics thus is $x|_{experim} \gg y|_{experim}$. This appears as a rather iffy scenario at present. Nevertheless it is mandatory to probe for oscillations with as much sensitivity as possible for three main reasons: (i) With oscillations being an intriguing quantum mechanical phenomenon their observation carries intrinsic intellectual value. (ii) We might be only one breakthrough in our computational control over nonperturbative dynamics away from making precise predictions. (iii) Last and most importantly: **CP** asymmetries that involve oscillations – see Sect. ?? below – would conclusively establish the existence of New Physics. Having an independent measurement of those oscillations would provide a most powerful validation of such asymmetries.

29.1.3 Time-dependent Rate for Incoherent D Decays

A search for mixing attempts to identify the process $|D^0\rangle \to |\overline{D}^0\rangle$ ($|\overline{D}^0\rangle \to |D^0\rangle$) by analyzing the decay products of a particle known to be created as a $|D^0\rangle$ ($|\overline{D}^0\rangle$). In practice, this means reconstructing the state $|f\rangle$ in an attempt to observe

$$|D^0\rangle \to |\overline{D}^0\rangle \to |f\rangle \tag{29.26}$$

The difficulty comes from the fact that for hadronic systems, the decay

$$|D^0\rangle \to |f\rangle\,, \tag{29.27}$$

can occur directly, without any mixing at all. Distinguishing Process (29.26) from (29.27) is the primary goal of D mixing searches, and it relies on the fact that the decay-time distribution of the final state $|f\rangle$ is different for the two processes. The most sensitivity of mixing will be found when the amplitude for process (29.27) is as small as possible, and therefore doubly Cabibbo-suppressed (DCS) decays are chosen for this type of analysis.

Let us define $A_f \equiv \langle f|\mathcal{H}|D^0\rangle$, $\overline{A}_f \equiv \langle f||\mathcal{H}|\overline{D}^0\rangle$ with $\rho_f \equiv \frac{\overline{A}_f}{A_f}$; and $A_{\overline{f}} \equiv \langle \overline{f}|\mathcal{H}|D^0\rangle$, $\overline{A}_{\overline{f}} \equiv \langle \overline{f}||\mathcal{H}|\overline{D}^0\rangle$ with $\overline{\rho}_{\overline{f}} \equiv \frac{A_{\overline{f}}}{\overline{A}_{\overline{f}}}$. Now the time-dependent *wrong sign* decay amplitude for states initially pure $|D^0\rangle$ ($|\overline{D}^0\rangle$) to decay to $|f\rangle$ ($|\overline{f}\rangle$) is given by (with $f = K^+\pi^-$ and define $|\overline{f}\rangle \equiv CP|f\rangle$)

$$A(|D^0_{\rm phys}(t) \to f) = \frac{q}{p}\overline{A}_f \left[\lambda_f^{-1} g_+(t) + g_-(t)\right], \tag{29.28}$$

and

$$A(|\overline{D}^0_{\rm phys}(t) \to \overline{f}) = \frac{p}{q}A_{\overline{f}} \left[\lambda_{\overline{f}} g_-(t) + g_+(t)\right], \tag{29.29}$$

where

$$\lambda_f \equiv \frac{q}{p}\frac{\overline{A}_f}{A_f} \equiv \frac{q}{p}\rho_f\ ,\ \lambda_{\overline{f}} \equiv \frac{q}{p}\frac{\overline{A}_{\overline{f}}}{A_{\overline{f}}} \equiv \frac{q}{p}\overline{\rho}_{\overline{f}}. \tag{29.30}$$

and

$$\frac{q}{p} = (1 + A_M)e^{i\phi}. \tag{29.31}$$

In order to describe the three types of CP violation in a convenient way, one can also parameterize the λ_f ($\lambda_{\overline{f}}$) as [235, 236]

$$\lambda_f \equiv \frac{q}{p}\frac{\overline{A}_f}{A_f} = \frac{(1 + A_M)}{\sqrt{R_D}(1 + A_D)}e^{i(\delta+\phi)}, \tag{29.32}$$

$$\lambda_{\overline{f}} \equiv \frac{q}{p}\frac{\overline{A}_{\overline{f}}}{A_{\overline{f}}} = \frac{\sqrt{R_D}(1 + A_M)}{(1 + A_D)}e^{-i(\delta-\phi)}, \tag{29.33}$$

where $|q|/|p| = (1 + A_M)$ and $|\overline{A}_f|/|A_f| = \sqrt{R_D}(1 + A_D)$, and δ is the strong phase difference between $\overline{A}_f$ and A_f. Here ϕ represents the convention-independent weak phase difference between the ratio of decay amplitudes and the mixing matrix. In Chapter 30, we will use these definition to describe the three types of CP violation in detail. In the limit of CP conservation, A_M, A_D and ϕ are all zero.

It is usual to normalize the *wrong sign* decay distributions to the integrated rate of *right sign* decays and to express time in units of the precisely measured D^0 mean lifetime, $\overline{\tau}_{D^0} = 1/\Gamma = 2/(\Gamma_1 + \Gamma_2)$. Therefore the time-dependent rates of production of the *wrong sign* final states relative to the integrated *right sign* states are:

$$r(t) = \left|\frac{q}{p}\right|^2 \left|\lambda_f^{-1} g_+(t) + g_-(t)\right|^2, \tag{29.34}$$

and

$$\overline{r}(t) = \left|\frac{p}{q}\right|^2 \left|\lambda_{\overline{f}} g_-(t) + g_+(t)\right|^2. \tag{29.35}$$

We will expand $r(t)$ and $\overline{r}(t)$ to second order in time for the modes where the ratio of the decay amplitudes $R_D = |A_f/\overline{A}_f|^2$ is very small (it is the ratio of DCSD rate and CFD rate).

29.2 Experimental Review

$D^0 - \overline{D}^0$ mixing and CP violation in charm sector have been searched for by various experimental facilities with different techniques. The principle production processes are $e^+e^- \to c\overline{c}$ at center of mass energy from threshold up to Z^0 boson peak, hadroproduction at both fixed-target experiments and the Fermilab Tevatron, photoproduction and so on. The cross sections vary from a few nb to microbarns for photoproduction, and to of order a millibarn at the Tevatron. However, the ratio of signal to background cross section are ranged from 1:1 in e^+e^- annihilation to 1:500 at the Tevatron as listed in table 29.1. D^0

Table 29.1: *Summary of Charm experiments nowadays with different techniques, luminosity, charm production cross section and ratio of signal to noise.*

Experiment	Beam	Lumin. ($\mathrm{cm}^{-2}\mathrm{s}^{-1}$)	Cross-Section	#events $c\overline{c}$ Per year	$\sigma(c\overline{c})/\sigma_{Total}$
BaBar	e^+e^- ($\Upsilon(4S)$)	3×10^{33}	1.3 nb	40×10^6	$\sim 1/5$
Belle	e^+e^- ($\Upsilon(4S)$)	3×10^{33}	1.3 nb	40×10^6	$\sim 1/5$
CLEO-c	e^+e^- ($\psi(3770)$)	2×10^{32}	6.4 nb	$6.4{\times}10^6$	~ 1
BES-III	e^+e^- ($\psi(3770)$)	1×10^{33}	6.4 nb	$32{\times}10^6$	~ 1
CDF	$p\overline{p}$ (1.9 TeV)		134 μb		$\sim 1/500$
LHC-b	$pp(\sqrt{s} = 14$ TeV)	2×10^{32}	1.0 mb	$1{\times}10^{11}$	$\sim 1/100$

mixing has not been observed yet, the most stringent limits on D mixing have been set by the Belle, *BaBar* and CLEO collaborations, analyzing hadronic D decays.

The techniques, which can be used to search for mixing, can be roughly divided into four classes: mixing in semi-leptonic decays, time-dependent measurements in wrong-sign decays to hadronic non-CP eigenstates, Decays to CP eigenstates and mixing measurements via Quantum Coherence at threshold.

29.2.1 Semileptonic Decays

The manifestation of D^0 mixing in semileptonic decays is relatively simple, since such transitions are flavor specific in the standard model or some of its extension. Because of the flavor specification of $D^0 \to l^+X^-$ and $\overline{D}^0 \to l^-X^+$, it is not necessary to study the time-dependent of D decay modes.

In semileptonic D decays, the wrong sign decay amplitudes $A_f = \overline{A}_{\overline{f}} = 0$. Then in the limit of weak mixing, where $|ix + y| \ll 1$, from Eq. (29.34), $r(t)$ is given by

$$r(t) = \left|\frac{q}{p}\right|^2 |g_-(t)|^2 \sim \frac{e^t}{4}(x^2+y^2)t^2 \left|\frac{q}{p}\right|^2, \tag{29.36}$$

In the limit of CP conservation, $r(t) = \overline{r}(t)$, and integrating Eq. (29.36 over all times gives

$$R_M = \int_0^\infty r(t)dt = \left|\frac{q}{p}\right|^2 \frac{x^2+y^2}{2+x^2+y^2} \simeq \frac{x^2+y^2}{2}, \tag{29.37}$$

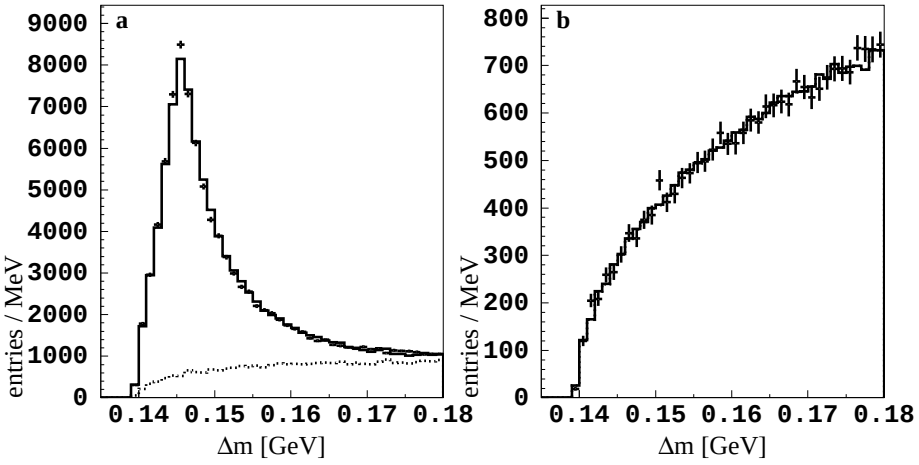

Figure 29.5: *(a)* ΔM *distribution for right-sign* $D^0 \to K^- l^+ \nu$ *candidate decays; (b) wrong-sign* $D^0 \to K^+ l^- \overline{\nu}$ *decays, from Belle using 253* fb^{-1} *of data [237]. The wrong-sign plot shows no visible signal above background.*

The semileptonic decay method usually suffers from large background (except at a τ-charm factory) due to the missing neutrino, which the final state is not fully reconstructed. The traditional method of looking for like sign $\mu^\pm\mu^\pm$ pairs is an example at fixed target experiments [238, 239, 240]. However, at an e^+e^- experiment there are enough kinematic constraints to infer the neutrino momentum. Specifically, momentum conservation prescribes $P_\nu = P_{CM} - P_{\pi_s Kl} - P_{\rm rest}$ [237], where P_{CM} is the four-momentum of the e^+e^- center-of-mass (CM) system, π_s, K, and l are daughters from decay $D^{*}+ \to D^0\pi_s \to \pi_s Kl\nu$, and $P_{\rm rest}$ is the four-momentum of the remaining particles in the event. In the B factory, the magnitude $|P_{\rm rest}$— is rescaled to satisfy $(P_{CM} - P_{\rm rest})^2 = m^2_{D^*}$, and after this rescaling the direction of $\overrightarrow{p_{\rm rest}}$ is adjusted to satisfy $P^2_\nu (= m^2_\nu) = 0$. One can also use information on the decay time to improve the sensitivity of the mixing [237]. The $\Delta M \equiv M_{\pi_s Kl\nu} - M_{Kl\nu}$ distribution for *right-sign* $D^0 \to K^- l^+ \nu$ and *wrong-sign* $D^0 \to K^+ l^- \nu$ samples are shown in Fig. 29.5 from Belle experiment using 253 $\rm fb^{-1}$ of data, which is the most stringent constraints currently. Table 29.2 is the summary of the experimental status of R_M measurements in semileptonic decays.

Table 29.2: *Results for* R_M *in* D^0 *semileptonic decays from PDG2006.*

Year	Experiment	Final states	R_M (90% C.L.)
2005	Belle [237]	$K^{(*)+}e^-\overline{\nu}$	$< 1.0^{-3}$
2005	CLEO [241]	$K^{(*)+}e^-\overline{\nu}$	$< 7.8 \times 10^{-3}$
2004	BaBar [242]	$K^{(*)+}e^-\overline{\nu}$	$< 4.2 \times 10^{-3}$
2002	FOCUS [243]	$K^+e^-\overline{\nu}$	$< 1.01 \times 10^{-3}$
1996	E791 [244]	$K^+e^-\overline{\nu}$	$< 5.0 \times 10^{-3}$

The best place to use the semileptonic method is probably in BES-III and CLEO-c near the charm threshold. The idea is to search for $e^+e^- \to \psi(3770) \to D^0\overline{D}^0 \to (K^- l^+\nu)(K^- l^+\nu)$ or $e^+e^- \to D^-\overline{D}^{*+} \to (K^+\pi^-\pi^-)(K^+ l^-\nu) + \pi_s$. The latter is probably

the only place where the semileptonic method does not suffer from a large background. It should have a very small background, as there is only one neutrino missing in the entire event, threshold kinematic constraints should provide clean signal as shown in Fig. **??**.

However, it has been point out that one can not claim a D^0 mixing signal based on the semileptonic decay alone (unless with information on the decay time of D^0 at B factory). Bigi [245] has pointed out that an observation of a signal on $D^0 \to l^- X^+$ establishes only that a certain selection rule is violated in the processes where the charm quantum number is changed, namely, the rule $\Delta C = -\Delta Q_l$ where Q_l denotes leptonic charge. This violation can occur either through $D^0 - \overline{D}^0$ mixing (with the unique attribute of the decay time-dependence of mixing), or through new physics beyond the SM (which could be independent of time). Nevertheless, one can always use this method to set upper limit for mixing.

29.2.2 Hadronic Final States

The *wrong-sign* hadronic decay modes can occur either through $D^0 - \overline{D}^0$ mixing or through DCSD as illustrated in Eqs. (29.26) and (29.27). The major complication for this method is the need to distinguish between DCSD and mixing. In principle, there are at least three ways to distinguish between DCSD and mixing candidates experimentally: (1) use the difference in the decay time-dependence [246, 247]; (2) use the possible difference in the resonance substructure between DCSD and mixing events on the Dalitz plot in three-body $D^0 \to K^+\pi^-\pi^0$ [248], or multi-body decays, like $D^0 \to K^+\pi^-\pi^+\pi^-$, etc.; (3) use the quantum correlation of the production and decay processes at $\psi(3770)$ peak [245, 249]. Method (1) is popular at B factory since the D^0 is highly boosted and so that the decay time information can be used. Method (2) requires knowledge of the structures of the DCSD decay on the Dalitz plots, which can be done at both B factory and a τ-charm factory. Method (3) can be done at BES-III at charm threshold region. In this subsection, we only discuss method (1), specifically.

According to Eq. (29.34), one get straightforwardly:

$$r(t) = \left|\frac{q}{p}\right| \left(\lambda_f^{-2} g_+^2(t) + \lambda_f^{-1} g_+(t) g_-^*(t) + (\lambda_f^{-1})^* g_+^*(t) g_-(t) + g_-^2(t)\right), \tag{29.38}$$

We can simplify Eq. (29.38) under the assumption of small mixing, $|ix + y| \ll 1$, and express

$$\begin{aligned} \lambda_f^{-2} g_+^2(t) &= |\lambda_f^{-1}|^2 \frac{e^{-t}}{2} \left[\cosh(yt) + \cos(xt)\right] \\ &\simeq |\lambda_f^{-1}|^2 e^{-t}, \end{aligned} \tag{29.39}$$

$$\begin{aligned} g_-^2(t) &= \frac{e^{-t}}{2} \left[\cosh(yt) - \cos(xt)\right] \\ &\simeq e^{-t} \left(\frac{x^2 + y^2}{4}\right) t^2, \end{aligned} \tag{29.40}$$

and

$$\begin{aligned}
&\lambda_f^{-1} g_+(t) g_-^*(t) + (\lambda_f^{-1})^* g_+^*(t) g_-(t) \\
&= \frac{e^{-t}}{2}\left(e^{-i(\delta+\phi)}(\sinh(yt) - i\sin(xt)) + e^{i(\delta+\phi)}(\sinh(yt) + i\sin(xt))\right) \\
&\simeq |\lambda_f^{-1}| e^{-t}(y\cos(\delta+\phi) - x\sin(\delta+\phi))t. \qquad (29.41)
\end{aligned}$$

If we define

$$y'_\pm \equiv y'\cos\phi \pm x'\sin\phi = y\cos(\delta \mp \phi) - x\sin(\delta \mp \phi), \qquad (29.42)$$

where

$$y' \equiv y\cos\delta - x\sin\delta\,,\; x' \equiv x\cos\delta + y\sin\delta, \qquad (29.43)$$

and combining Eq. (29.32), (29.39), (29.40) and (29.41), in the limit of CP conservation ($A_D = 0$, $A_M = 0$ and $\phi = 0$), we obtain the standard form for the time-dependent decay rate, including D mixing:

$$r(t) = \overline{r}(t) = e^{-t}\left(R_D + \sqrt{R_D}y't + \frac{1}{2}R_M t^2\right), \qquad (29.44)$$

the above wrong-sign decay rate includes three components: one from the DCSD, a second from mixing, and a third from the interference between the first two. The time-integrated wrong-sign rate relative to the integrated right-sign rate is

$$R_{WS} = \int_0^\infty r(t)dt = R_D + \sqrt{R_D}y' + \frac{1}{2}R_M\,, \qquad (29.45)$$

A shown in Eq. (29.44), D mixing is characterized in the decay rate by a small deviation away from a pure exponential. In order to have the most sensitivity to $(x^2 + y^2)$, a decay channel for which R_D is relatively small is desired. The analysis technique benefits from the ability to compare the signal distribution, given by Eq. (29.44), to the CF decay distribution, which may be treated as pure exponential. In this way, systematic bias is significantly limited.

The ratio R_{WS} is the most readily accessible experimental quantity. Table 29.3 gives recent measurement of R_{WS} in $D^0 \to K^+\pi^-$ decay. The average of these results, $R_{WS} = (0.376 \pm 0.009)\%$ [**?**].

The interference causes the measured x and y to be rotated through an angle δ, the phase difference between the DCS and CF decay processes. By measuring the time dependence of the decay rate it is possible to sort out the mixing from the DCS decay. At B factories and CLEO experiments, wrong-sign candidate events of the types $D^0 \to K^+\pi^-$ and $\overline{D}^0 \to K^-\pi^+$ are selected by requiring that the soft π_s from the D^* decay and the daughter K of the D^0 to have identical charge (wrong-sign tag). In order to determine the wrong-sign and right-sign yields, two powerful distinguishing variables are selected at Belle experiment, $M_{K\pi}$ and the released energy $Q \equiv M^* - M_{K\pi} - m_{\pi_s}$, where M^* is the reconstructed mass of the $K^+\pi^-\pi_s^+$ system, $M_{K\pi}$ is the reconstructed mass of $K^+\pi^-$ system, and m_{π_s} is the charged pion mass. While, at BaBar and CLEO experiments, they

Table 29.3: *Results for R_{WS} and A_D in $D^0 \to K^+\pi^-$, if assume that there is no mixing and CP violation in DCSD decay is allowed.*

Experiments	Techniques	Assumption	R_{WS} ($\times 10^{-3}$)	$A_D(\%)$
Belle [247]	$e^+e^- \to \Upsilon(4S)$	No mix	$3.77 \pm 0.08 \pm 0.05$	–
FOCUS [251]	γ BeO	No mix	$4.29 \pm 0.63 \pm 0.28$	$18.0 \pm 14.0 \pm 4.1$
BaBar [246]	$e^+e^- \to \Upsilon(4S)$	No mix	$3.57 \pm 0.22 \pm 0.27$	$9.5 \pm 6.1 \pm 8.3$
CLEO [236]	$e^+e^- \to \Upsilon(4S)$	No mix	$3.32^{+0.63}_{-0.65} \pm 0.40$	$2.0^{+19.0}_{-20.0} \pm 1.0$
CDF [252]	$p\overline{p} \to c\overline{c}$	no mix	$4.05 \pm 0.21 \pm 0.11$	–

Table 29.4: *Limits on x'^2 and y', both 95% C.L. for case where CP violation is allowed and also where it is not allowed.*

Experiment	$x'^2(\times 10^{-3})$ (95% CL)		$y'(\times 10^{-3})$ (95% CL)	
	CPV	No CPV	CPV	No CPV
BaBar [246]	2.2	2.0	-56 $< y' <$ 39	-27$< y' <$ 22
FOCUS [251]	0.80	0.83	-120 $< y' <$ 67	-72$< y' <$ 41
CLEO [236]	0.82	0.78	-58 $< y' <$ 10	-52$< y' <$ 2
Belle [247]	0.72	0.72	-28 $< y' <$ 21	-9.9$< y' <$ 6.8

used mass difference $\delta m = M^* - M_{K\pi}$. Figure 29.6 shows the $M_{K\pi}$ and Q distributions superimposed with projections of the fit result. To detect a deviation from an exponential decay in wrong-sign events, a likelihood fit to the distribution of the reconstructed proper decay time t is perform for each experiment. The likelihood fit includes a signal and a background component and models each as the convolution of a decay-time distribution and a resolution function. As an example, the left plot in Fig. 29.7 shows us the wrong-sign $D^0 \to K^+\pi^-$ decay-time distribution and fit projections from Belle experiment.

Limits on x'^2 and y' from several experiments are listed in Table 29.4 and x'^2 and y'. The limits are somewhat more restrictive on y' when CP violation is not allowed, while those on x'^2 hardly change. While no experiment claims an effect, it is interesting that the Belle result is consistent with no mixing only at 3.9% C.L. [247]. The right plot in Fig. 29.7 shows us the 95% C.L. region in the x'^2-y' plane by using a frequentist technique based on toy Monte Carlo simulation.

The mixing has also been searched for the wrong-sign multibody final states [253, 254, 255] $K^+\pi^-\pi^0$ and $K^+\pi^-\pi^+\pi^-$. Using 281 fb^{-1} of data, Belle collaboration have done a time-integrated analysis, and measured the time-independent ratio of wrong-sign to right-sign decays. The results are $R_{WS} = (0.229 \pm 0.015^{+0.013}_{-0.009})\%$ for the $D^0 \to K^+\pi^-\pi^0$ and $R_{WS} = (0.320 \pm 0.018^{+0.018}_{-0.013})\%$ for the $D^0 \to K^+\pi^-\pi^+\pi^-$.

Recently, BaBar collaboration reported a measurement of mixing rate R_M in the decay of $D^0 \to K^+\pi^-\pi^0$ with a time-dependent analysis [248]. There are two key motivations to select $D^0 \to K^+\pi^-\pi^0$: (1) one expect the Dalitz-plot structure of DCS decay differs from that of CF decay, we note that DCS decays proceed primarily through the resonance $D^0 \to K^{*+}\pi^-$, $K^{*0}\pi^0$, while CF decays proceed primarily through the resonance $D^0 \to K^-\rho^+$.

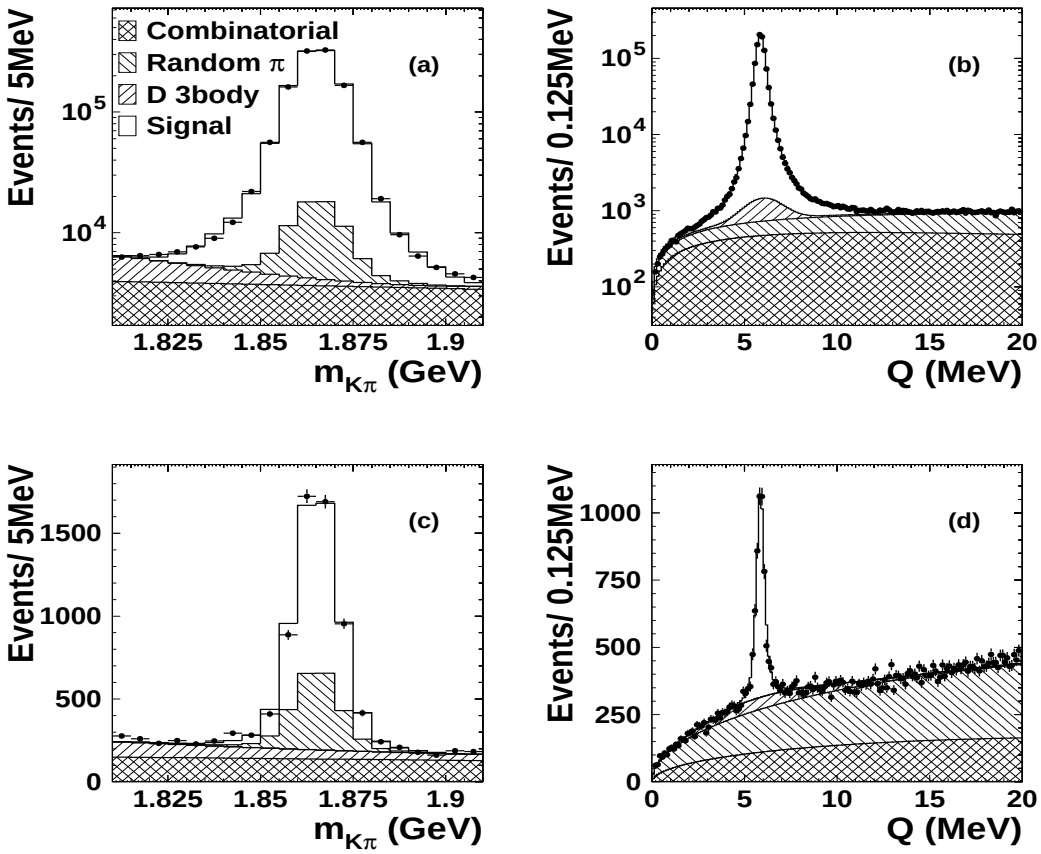

Figure 29.6: *The distribution for (a) Right-sign $M_{K\pi}$ with $0 < Q < 20$ MeV, (b) Right-sign Q with 1.81 GeV/c^2< $M_{K\pi} < 1.91$ GeV/c^2, (c) Wrong-sign $M_{K\pi}$ with $5.3 < Q < 6.5$ MeV, and (d) Wrong-sign Q with $1.845 < m_{K\pi} < 1.885$ GeV/c^2. Note that the wrong-sign plots are shown for a 3σ signal interval in Q and $MK\pi$, respectively. Superimposed on the data (points with error bars) are projections of the $M_{K\pi} - Q$ fit. The results are from Belle experiment with 400 fb^{-1} of data.*

The sensitivity to R_M measurement may be increased by selecting regions of the Dalitz plot where CF decay contributes with a large amplitude relative to the corresponding DCS decay amplitude. (2) The time-integrated mixing rate $R_M = (x^2+y^2)/2$ is independent of the decay mode and is expected to be consistent among mixing measurement. Figure 29.8 shows us the Dalitz plots for CF and DCS decay. The CF Dalitz plot is qualitatively different from the wrong-sign Dalitz plot, which is assumed to contain primarily DCS contributions. While CF decays proceed primarily through the resonance $D^0 \to K^-\rho^+$, DCS decays proceed primarily through the resonance $D^0 \to K^{*+}\pi^-$. So the particular regions of the phase space (i.e., the Dalitz plot) are selected by removing the K^* resonance. In the limit of CP conservation, the time-dependent ratio of wrong-sign to right-sign is

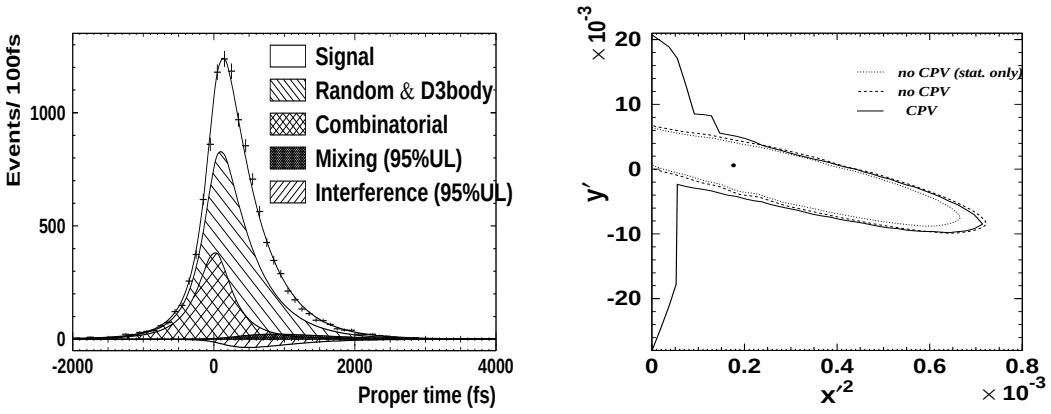

Figure 29.7: *Left: wrong-sign $D^0 \to K^+\pi^-$ decay-time distribution and fit projections. Right: 95% C.L. region for x'^2, y'. From Belle using 400 fb^{-1} of data [247].*

expressed approximately as:

$$R_{WS} = \tilde{R}_D \quad + \quad \alpha\sqrt{\tilde{R}_D}\tilde{y}'\,t + \frac{1}{2}R_M t^2 \qquad (29.46)$$
$$0 \leq \alpha \leq 1\,,$$

where the tilde indicates quantities that have been integrated over any choice of phase space regions. Here $\tilde{R}_D$ is the integrated DCS ratio of DCS decays to CF decays; $\tilde{y}' = y\cos\tilde{\delta} - x\sin\tilde{\delta}$, $\tilde{\delta}$ is an unknown integrated strong-phase difference between the CF and the DCS decay amplitudes; α is a suppression factor that accounts for strong-phase variation over the regions. The time-integrated mixing rate R_M is independent of decay mode. By fitting the proper time distribution, they get the results $R_M = (0.023^{+0.018}_{-0.014} \pm 0.004)\%$ and $\tilde{R}_D = (0.164^{+0.026}_{-0.022} \pm 0.012)\%$ by assuming CP invariance. The upper limit is set to be $R_M < 0.054\%$ at 95% confidence level. They conclude that the observed data are consistent with no mixing at the 4.5% confidence level. By using a similar method and idea, BaBar experiment also measured the time-integrated mixing rate R_M in $D^0 \to K^+\pi^-\pi^+\pi^+$ decay mode. Assuming CP conservation, they got $R_M = (0.019^{+0.016}_{-0.015} \pm 0.002)\%$, and $R_M < 0.048\%$ at 95% C.L.. Furthermore, they combined results from both decay modes, and found that $R_M = (0.020^{+0.011}_{-0.010})\%$ and $R_M < 0.042\%$ at 95% C.L. which is the best limit with current data. The combined data sets are consistent with the no-mixing hypothesis with 2.1% confidence.

29.2.3 D^0 Decays to CP Eigenstates

D^0 mixing parameters can be measured by comparing the lifetimes extracted from the analysis of D decays into the CP-even and CP-odd final states. When the final state is CP eigenstate f (i.e., $|\overline{f}\rangle \equiv CP|f\rangle = \pm|f\rangle$), such as K^+K^-, $\pi^+\pi^-$ and $K_S\pi^0$, there is no strong phase difference between $\overline{A}_f$ and A_f. Assuming $|\overline{A}_f| = |A_f|$ (no direct CP violation), $\lambda_f = -|q|/|p|e^{i\phi}$ and $\lambda_{\bar{f}} = -|p|/|q|e^{-i\phi}$, where ϕ is the weak phase difference.

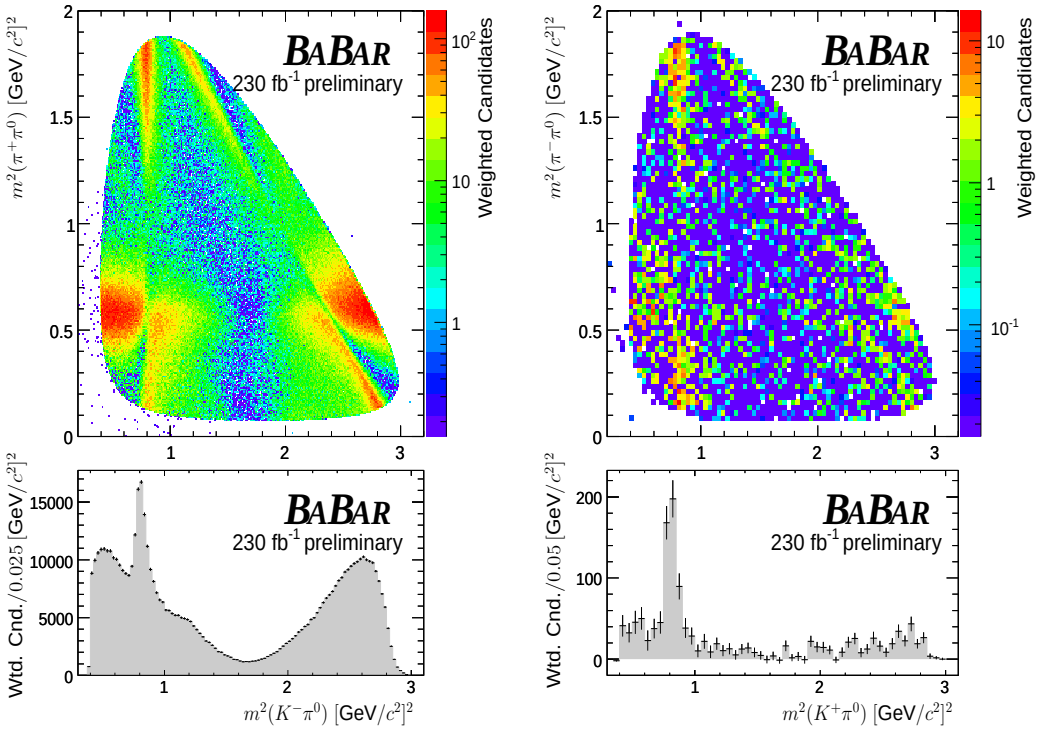

Figure 29.8: *Dalitz plot and one-dimensional projection onto $m^2_{K\pi^0}$ for CF decays (left) and DCS decays (right). The shaded histograms in the lower plots are projections of the Dalitz plots above them, with error bars superimposed. The data are from BaBar with 230 fb^{-1}.*

Inserting these terms into Eqs. (29.34) and (29.35) gives

$$R(D^0 \to K^+K^-) \simeq |A_{K^+K^-}|^2 e^{-t} e^{-|q/p|(y\cos\phi - x\sin\phi)t}, \tag{29.47}$$

and

$$R(\overline{D}^0 \to K^+K^-) \simeq |A_{K^+K^-}|^2 e^{-t} e^{-|p/q|(y\cos\phi + x\sin\phi)t}. \tag{29.48}$$

Eqs. (29.47) and (29.48) imply that the measured D^0 and $\overline{D}^0$ inverse lifetimes are slightly different each other. We define

$$y_{CP} = \frac{\tau_{D^0\to K^-\pi^+}}{\tau_{D^0\to K^+K^-}} - 1 = \frac{q}{p}(y\cos\phi - x\sin\phi), \tag{29.49}$$

for D^0 decays, and for $\overline{D}^0$ decays, it is

$$y_{CP} = \frac{\tau_{\overline{D}^0\to K^+\pi^-}}{\tau_{\overline{D}^0\to K^+K^-}} - 1 = \frac{p}{q}(y\cos\phi + x\sin\phi). \tag{29.50}$$

For $|q/p| = 1$, i.e., no CP violation in mixing, $y_{CP} = y\cos\phi$ for equal number of D^0 and $\overline{D}^0$ decays together. If also $\phi = 0$ (no CP violation), $y_{CP} = y$.

One can also combine the two $D \to K^+K^-$ modes. To understand the consequences of such an analysis, one has to consider the relative weight of D^0 and $\overline{D}^0$ in the sample. Let us define $A_{\rm prod}$ as the production asymmetry of D^0 and $\overline{D}^0$:

$$A_{\rm prod} = \frac{N(D^0) - N(\overline{D}^0)}{N(D^0) + N(\overline{D}^0)}. \tag{29.51}$$

Then

$$\begin{aligned} y_{CP} &= \frac{\tau_{D^0\to K^-\pi^+}}{\tau_{D\to K^+K^-}} - 1 \\ &= y\cos\phi \left[\frac{1}{2}\left(\left|\frac{p}{q}\right| + \left|\frac{q}{p}\right|\right) + \frac{A_{\rm prod}}{2}\left(\left|\frac{p}{q}\right| - \left|\frac{q}{p}\right|\right)\right] \\ &\quad -x\sin\phi \left[\frac{1}{2}\left(\left|\frac{p}{q}\right| - \left|\frac{q}{p}\right|\right) + \frac{A_{\rm prod}}{2}\left(\left|\frac{p}{q}\right| + \left|\frac{q}{p}\right|\right)\right], \end{aligned} \tag{29.52}$$

Table 29.5: Summary of y_{CP}results.

Experiment	y_{CP}
FOCUS [?]	$3.4 \pm 1.4 \pm 0.7$
CLEO [?]	$-1.2 \pm 2.5 \pm 1.4$
Belle, untagged [?]	$-0.5 \pm 1.0 \pm 0.8$
Belle, tagged [?]	$1.2 \pm 0.7 \pm 0.4$
BaBar [?]	$0.8 \pm 0.4^{+0.5}_{-0.4}$

The y_{CP} is determined from the slope of the decay-time distribution in sample of $D^0 \to K^-\pi^+$, which is an equal mixture of CP-even and CP-odd final states, and $D^0 \to K^+K^-$ or $\pi^+\pi^-$, which are even final states. An unbinned maximum likelihood fit to the distribution of the reconstructed proper time t of the D^0 candidates is performed. To date, five experiments have been measured y_{CP} as listed in Table 29.5. The most precise value is from BaBar using 91 fb^{-1} of date. To increase statistics, BaBar used both K^+K^- and $\pi^+\pi^-$ decays, and in addition, the $D^0 \to K^+K^-$ analysis used both a large inclusive D^0 sample and smaller, higher purity sample in which the D^0 is required to originate from $D^{*+} \to D^0\pi_s^+$. The respective decay time distributions are shown in Fig. 29.9. BaBar also measured $\Delta Y \equiv (\tau^+ - \tau^-)/(\tau^+ + \tau^-) \times \tau_{K^-\pi^+}/\langle\tau\rangle$, where τ^+ (τ^-) is the lifetime for $D^0 \to K^+K^-$ ($\overline{D}^0 \to K^+K^-$) and $\langle\tau\rangle = (\tau^+ + \tau^-)/2$. For $|q/p| = 1$, $\Delta Y = x\sin\phi$. The result is $\Delta Y = (-0.8 \pm 0.6 \pm 0.2)\%$, which indicates that either x or ϕ is small.

Since it needs to fit proper time distribution, this method can not applied to the BES-III and CLEO-c experiments near the threshold of open charm.

29.2.4 Dalitz Plots

At present, the only time-dependent analysis is done by CLEO in $D^0 \to K_S\pi^+\pi^-$ decay mode. They consider a self-conjugate final state that is not CP eigenstate due to the

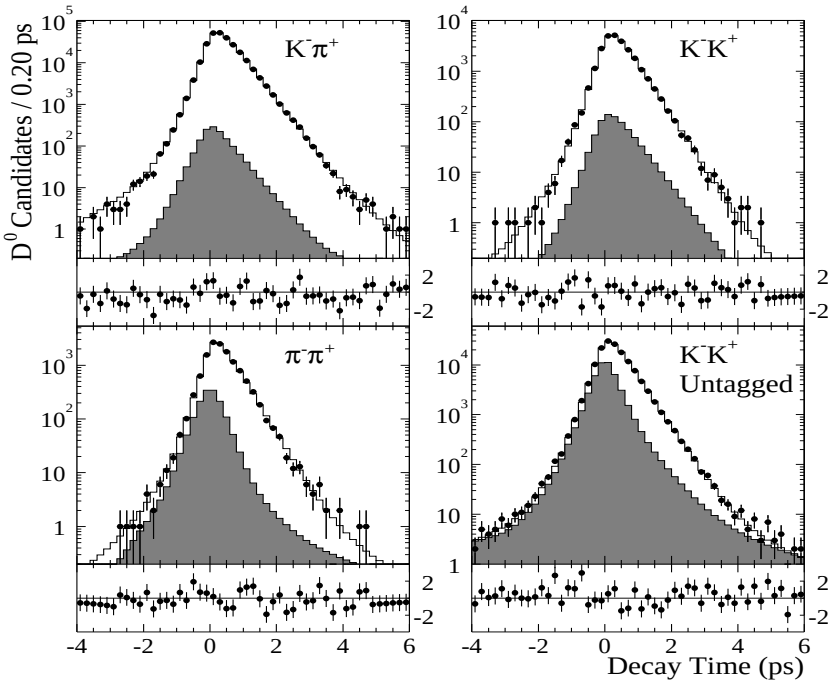

Figure 29.9: *Decay time distributions for CF $D^0 \to K^-\pi^+$ (upper left), $D^0 \to K^+K^-$ (upper right), $D^0 \to \pi^+\pi^-$ (lower left), and $D^0 \to K^+K^-$ selected without using a D^{*0} tag (lower right), from BaBar using 91 fb^{-1} of data [?]. The higtograms are fit results superimposed on the data (dotted histograms). The shaded histograms is the portion of the sample assigned by the fit to the background. The points presented below the histograms are the difference between data and dit divided by the statistical error with error bars of unit length.*

substructures with either $L = 0$ (CP-even) or $L = 1$ (CP-odd) in the three body decay. The decay rate to $K_S\pi^+\pi^-$ with ($m^2_{K_S\pi^-}$, $m^2_{\pi^+\pi^-}$) at time t of a particle tagged as $|D^0\rangle$ at $t = 0$ is

$$d\Gamma(m^2_{K\pi}, m^2_{\pi\pi}, t) = \frac{1}{256\pi^3 M^3}|\mathcal{M}|^2 dm^2_{K\pi} dm^2_{\pi\pi}, . \tag{29.53}$$

where the matrix element is defined as $\mathcal{M} = \langle f|H|D^0(t)\rangle$, and $\langle f| = \langle K_S\pi^+\pi^-(m^2_{K_S\pi^-}, m^2_{\pi^+\pi^-})|$. The $|D^0(t)\rangle$ is given in Eq. (29.11).

The decay channels can be collected into those which are CP even or CP odd (with amplitudes Amp_+ or Amp_-) and to those which are D^0 or $\overline{D}^0$ flavor eigenstates (with amplitudes Amp_f or $\overline{\mathrm{Amp}}_f$):

$$\langle f|\mathcal{H}|D_{+,-}\rangle = \sum a_j e^{i\delta_j}\mathcal{A}^j_{+,-} = p\mathrm{Amp}_{+,-}\,; \tag{29.54}$$

$$\langle \overline{f}|\mathcal{H}|D_{+,-}\rangle = \sum a_j e^{i\delta_j}\overline{\mathcal{A}}^j_{+,-} = q\overline{\mathrm{Amp}}_{+,-}\,; \tag{29.55}$$

$$\langle f|\mathcal{H}|D^0\rangle = \sum a_j e^{i\delta_j}\mathcal{A}^j = \mathrm{Amp}_f\,; \tag{29.56}$$

$$\langle \overline{f}|\mathcal{H}|\overline{D}^0\rangle = \sum a_j e^{i\delta_j}\overline{\mathcal{A}}^j = p\overline{\mathrm{Amp}}_{\overline{f}}; \tag{29.57}$$

where a_j and δ_j are the explicitly CP conserving amplitudes and relative strong phases (in Ref. [?], they fix $a_\rho = 1$, $\delta_\rho = 0$, all the other strong phases are relative to ρ resonance) for the jth quasi-two-body state. $\mathcal{A}^j_{+,-} = \mathcal{A}^j_{+,-}(m^2_{K_S\pi^-}, m^2_{\pi^+\pi^-})$ is the Breit-Wigner amplitude for resonance j with D decay to $CP = +$ or $CP = -$ quasi-two-body contributions. In Ref. [?], CLEO experiment considered the following ten modes: $K^{*-}\pi^+$, $K_0^*(1430)^-\pi^+$, $K_2^*(1430)^-\pi^+$, $K^*(1680)^-\pi^+$, $K_S\rho$ $K_S\omega$, $K_Sf_0(980)$, $K_Sf_2(1270)$, $K_Sf_0(1370)$, and the "wrong-sign" $K^{*+}\pi^-$ plus a small non-resonant component. Collecting terms with similar time dependence and combining Eqs. (29.11) and (29.12), one can find

$$\begin{aligned}
\mathcal{M} &= \langle f|\mathcal{H}|D^0(t)\rangle = \frac{1}{2p}(\langle f|\mathcal{H}|D_1(t)\rangle + \langle f|\mathcal{H}|D_2\rangle) \\
&= \frac{1}{2p}(\langle f|\mathcal{H}|(pD^0 + q\overline{D}^0)\rangle e_1(t) + \langle f|\mathcal{H}|(pD^0 - q\overline{D}^0)\rangle e_2(t)) \\
&= \frac{1}{2p}([p(\mathrm{Amp}_f + \mathrm{Amp}_+) + q(\overline{\mathrm{Amp}}_f + \overline{\mathrm{Amp}}_+)]e_1(t) \\
&\quad +[p(\mathrm{Amp}_f + \mathrm{Amp}_-) - q(\overline{\mathrm{Amp}}_f + \overline{\mathrm{Amp}}_-)]e_2(t)) \\
&= \frac{1}{2}([(1+\chi_f)\mathrm{Amp}_f + (1+\chi_+)\mathrm{Amp}_+]e_1(t) \\
&\quad +[(1-\chi_f)\mathrm{Amp}_f + (1-\chi_-)\mathrm{Amp}_-]e_2(t)) \\
&\equiv e_1(t)A_1 + e_2A_2\,, \qquad (29.58)
\end{aligned}$$

and

$$\begin{aligned}
\overline{\mathcal{M}} &= \langle \overline{f}|\mathcal{H}|\overline{D}^0(t)\rangle = \frac{1}{2q}(\langle \overline{f}|\mathcal{H}|D_1(t)\rangle - \langle \overline{f}|\mathcal{H}|D_2\rangle) \\
&= \frac{1}{2}([(\chi_{\overline{f}}^{-1}+1)\overline{\mathrm{Amp}}_{\overline{f}} + (\chi_+^{-1}+1)\overline{\mathrm{Amp}}_+]e_1(t) \\
&\quad -[(\chi_{\overline{f}}^{-1}-1)\overline{\mathrm{Amp}}_{\overline{f}} + (\chi_-^{-1}-1)\overline{\mathrm{Amp}}_-]e_2(t)) \\
&\equiv e_1(t)\overline{A}_1 + e_2\overline{A}_2\,, \qquad (29.59)
\end{aligned}$$

for D^0 and $\overline{D}^0$, respectively. CLEO experiment defines

$$\chi_f = \frac{q}{p}\frac{\overline{Amp}_f}{\mathrm{Amp}_f} = \left|\frac{\overline{Amp}_f}{\mathrm{Amp}_f}\right|(1+A_M)e^{i(\delta+\phi)} \qquad (29.60)$$

$$\chi_{\overline{f}} = \frac{q}{p}\frac{\overline{Amp}_{\overline{f}}}{\mathrm{Amp}_{\overline{f}}} = \left|\frac{\overline{Amp}_{\overline{f}}}{\mathrm{Amp}_{\overline{f}}}\right|(1+A_M)e^{-i(\delta-\phi)} \qquad (29.61)$$

$$\chi_\pm = \pm\frac{q}{p}\frac{\overline{Amp}_\pm}{\mathrm{Amp}_\pm} = \pm\left|\frac{\overline{Amp}_\pm}{\mathrm{Amp}_\pm}\right|(1+A_M)e^{\pm i\phi)}\,, \qquad (29.62)$$

where δ is the relative strong phase between D^0 and $\overline{D}^0$ to $K_S\pi^+\pi^-$, and in the limit of CP conservation, the real CP-violating parameters, A_D and ϕ, are zero. Squaring the amplitude and factoring out the time-dependent yields

$$|\mathcal{M}|^2 = |e_1(t)|^2|A_1|^2 + |e_2(t)|^2|A_2|^2 + 2Re[e_1(t)e_2^*(t)A_1A_2^*]\,. \qquad (29.63)$$

$$|\overline{\mathcal{M}}|^2 = |e_1(t)|^2|\overline{A}_1|^2 + |e_2(t)|^2|\overline{A}_2|^2 + 2Re[e_1(t)e_2^*(t)\overline{A}_1\overline{A}_2^*]\,. \tag{29.64}$$

The time-dependent terms are given explicitly by

$$|e_1(t)|^2 = e^{\Gamma_1 t} = e^{-\Gamma(1-y)t} \tag{29.65}$$

$$|e_2(t)|^2 = e^{\Gamma_2 t} = e^{-\Gamma(1+y)t} \tag{29.66}$$

$$\begin{aligned} e_1(t)e_2^*(t) &= e^{-\lambda_{D_1}t}e^{+\lambda_{D_2}t} = e^{-\Gamma(1+ix)t} \\ &= e^{\Gamma t}(\cos(\Delta m t) - i\sin(\Delta m t)) \end{aligned} \tag{29.67}$$

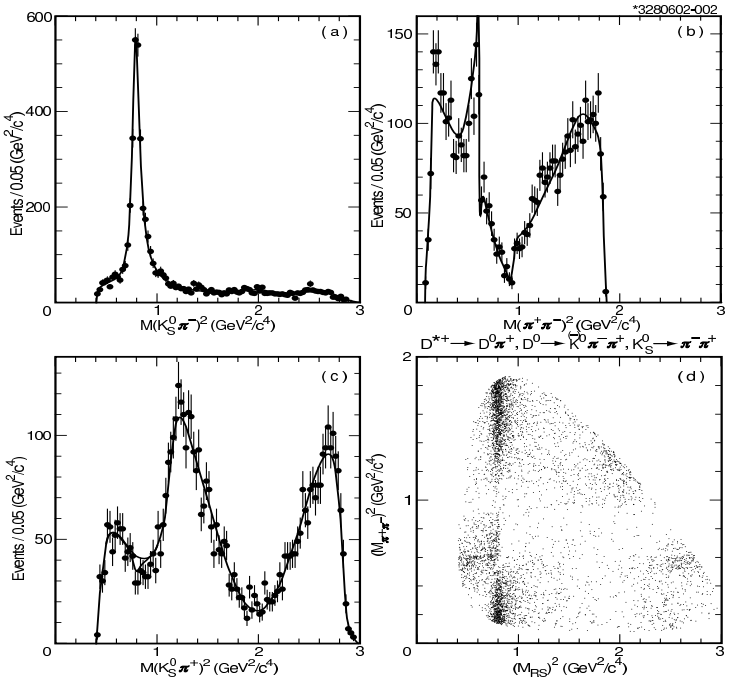

Figure 29.10: *Dalitz plot (lower right) and projections (lower left, upper plots) for* $D^0 \to K^0_S\,\pi^+\pi^-$ *decays, from CLEO using 9.0* fb^{-1} *of data.[?]*

Experimentally, y modifies the lifetime of certain contributions to the Dalitz plot while x introduces a sinusoidal rate variation. Then, $|\mathcal{M}|^2$ can be expressed as

$$\begin{aligned} |\mathcal{M}|^2 &= |A_1|^2 e^{-\Gamma(1-y)t} + |A_2|^2 e^{-\Gamma(1+y)t} \\ &\quad +2e^{\Gamma t}(ReA_1A_2^*\cos(\Delta m t) + ImA_1A_2^*\sin(\Delta m t)) \end{aligned} \tag{29.68}$$

Using above probability density function, CLEO does an unbinned maximum likelihood fit to the Dalitz plot and the time t distribution to determine a_j, δ_j, x and y. There is systematic uncertainty arising from the decay model, i.e., one must decide which intermediate states to include in the fit. Eq. (29.68) depends linearly on x ($x < 1$) and is therefore sensitive to the sign of x.

Table 29.6: *Limits on mixing and CP violation parameters from a t-dependent fit to the* $D^0 \to K^0_S \pi^+\pi^-$ *Dalitz plot, from CLEO using 9.0* fb^{-1}*.[?] The errors are statistical, experimental systematic, and modelling systematic, respectively.*

Fit	**Param.**	**Fit Result (%)**	**95% C.L. Inter. (%)**
No CPV	x	$1.8^{+3.4}_{-3.2} \pm 0.4 \pm 0.4$	$(-4.7, 8.6)$
	y	$-1.4^{+2.5}_{-2.4} \pm 0.8 \pm 0.4$	$(-6.3, 3.7)$
CPV Allowed	x	$2.3^{+3.5}_{-3.4} \pm 0.4 \pm 0.4$	$(-4.5, 9.3)$
	y	$-1.5^{+2.5}_{-2.4} \pm 0.8 \pm 0.4$	$(-6.4, 3.6)$
	ϵ	$1.1 \pm 0.7 \pm 0.4 \pm 0.2$	$(-0.4, 2.4)$
	ϕ	$(5.7 \pm 2.8 \pm 0.4 \pm 1.2)^\circ$	$(-0.3^\circ, 11.7^\circ)$

The time-dependent Dalitz analysis techniques are developed by CLEO [**?**], and their results based on 9.0 fb^{-1} of data have not yet been superseded. To minimize backgrounds, the D^0 candidate is required to originate from $D^{*+} \to D^0\pi^+$. The final Dalitz plot sample contains 5299 events with only $(2.1 \pm 1.5)\%$ background as shown in Fig. 29.10. The fit results are listed in Table 29.6; the 95% C.L. intervals corresponding to the values at which $-2ln\updownarrow$ rises by 3.84 units, where $\mathcal{L}$ is the likelihood function. CP violation is included in the fit

29.3 Measurements on $\psi(3770)$ peak

At BESIII, the $\psi(3770)$ decays will provide another opportunity to search for $D^0 - \overline{D}^0$ mixing and understand the source of CP violation in Charm system. The amplitude for $\psi(3770)$ decaying to $D^0\overline{D}^0$ is $\langle D^0\overline{D}^0|H|\psi(3770)\rangle$, and the $D^0\overline{D}^0$ pair system is in a state with charge parity $C + -1$, which can be defined as

$$|D^0\overline{D}^0\rangle^{C=-1} = \frac{1}{\sqrt{2}}[|D^0\rangle|\overline{D}^0\rangle - |\overline{D}^0\rangle D^0\rangle]. \tag{29.69}$$

Although there is weak current contribution in $\psi(3770) \to D^0\overline{D}^0$ decay, which may not conserve charge parity, the $D^0\overline{D}^0$ pair can not be in a state with $C = +1$. The reason is that the relative orbital angular momentum of $D^0\overline{D}^0$ pair must be $l = 1$ because angular momentum conservation. A boson-pair with $l = 1$ must be in an anti-symmetric state, the anti-symmetric state of particle-anti-particle pair must be in a state with $C = -1$. The $D^0\overline{D}^0$ will therefore be in an entangled state with the same quantum numbers as the parent resonance.

In general, as shown in Ref. [256], a $D^0\overline{D}^0$ pair produced through a virtual photon in the reaction $e^+e^- \to D^0\overline{D}^0 + m\gamma + n\pi^0$ is in a $C = (-1)^{m+1}$ state. Thus, as the $\psi(3770)$, where no additional fragmentation particles are produced, there is only $C = -1$, while at higher energies above $D^*\overline{D}$ threshold, we can access $C = -1$ or $C = +1$ eigenstate, such as $e^+e^- \to \psi(4140) \to \gamma(D^0\overline{D}^0)_{C=+1}or\pi^0(D^0\overline{D}^0)_{C=-1}$.

We now consider decays of these correlated systems into various final states, searching in particular for interference effects depending on δ. In all cases, we integrate with respect to proper time, since vertex separation in a symmetric e^+e^- "charm factory" is likely to be problematic. Xing [257] and Gronau *et al.* [258] have considered time-integrated decays into correlated pairs of states, including some effects of a non-zero final state phase difference. In Ref. [258], Gronau *et al.* derived general expressions for time-integrated decay rates into a pair of final states f_1 and f_2, from $C = -1$ and $C = +1$ $D^0\overline{D}^0$ states:

$$\Gamma^{C=-1}(f_1, f_2) = \frac{1}{2}|a^-|^2\left[\frac{1}{1-y^2} + \frac{1}{1+x^2}\right] + \frac{1}{2}|b^-|^2\left[\frac{1}{1-y^2} - \frac{1}{1+x^2}\right], \tag{29.70}$$

$$\begin{aligned}\Gamma^{C=+1}(f_1, f_2) &= \frac{1}{2}|a^+|^2\left[\frac{1+y^2}{(1-y^2)^2} + \frac{1-x^2}{(1+x^2)^2}\right] \\ &+ \frac{1}{2}|b^-|^2\left[\frac{1+y^2}{(1-y^2)^2} - \frac{1}{(1-x^2)^2}\right] \\ &+ 2\mathcal{R}e\left\{a^{+*}b^+\left[\frac{y}{(1-y^2)^2} + \frac{ix}{(1+x^2)^2}\right]\right\},\end{aligned} \tag{29.71}$$

where

$$a^\pm = \langle f_1|D^0\rangle\langle f_2|\overline{D}^0\rangle \pm \langle f_1|\overline{D}^0\rangle\langle f_2|D^0\rangle, \tag{29.72}$$

$$b^\pm = \langle f_1|D^0\rangle\langle f_2|D^0\rangle \pm \langle f_1|D^0\rangle\langle f_2|D^0\rangle, \tag{29.73}$$

they can be easily generalized allowing for CP violation [258]:

$$a^{\pm} = \frac{p}{q} A_1 A_2 (\lambda_2 \pm \lambda_1), \tag{29.74}$$

$$b^{\pm} = \frac{p}{q} A_1 A_2 (1 \pm \lambda_1 \lambda_2), \tag{29.75}$$

where

$$A_i \equiv \langle f_i | D^0 \rangle, \quad \overline{A}_i \equiv \langle f_i | \overline{D}^0 \rangle, \quad \lambda_i \equiv \frac{q}{p} \frac{\overline{A}_i}{A_i}. \tag{29.76}$$

The definition in above Equation had been discussed in detail in Section 29.1.3.

As in Refs. [258, 257, 259, 260], we consider the following categories of D^0 and $\overline{D}^0$ final states:

- Hadronic final states, f or $\overline{f}$, but not CP eigenstates, such as $K^-\pi^+$, which is produced via CF D^0 transitions or DCS $\overline{D}^0$ transitions;
- Semileptonic or pure leptonic final states, l^+ or l^-, which, in the absence of mixing, tag unambiguously the flavor of the parent D;
- CP-even (S_+) and CP-odd (S_-) eigenstates, respectively.

We will discuss different final states by assuming CP conservation. Taking into account that x, $y \ll 1$, keeping terms up to order x^2, y^2 and R_D (R_D is the ratio between DCS and CF decay rate as defined in Eq. (29.33) in the expressions, neglecting CP violation in decay and mixing, one got the following results for various cases [258]

$C = -1$ $D^0\overline{D}^0$ states:

- $(K^-\pi^+)(K^-\pi^+)$.

$$\Gamma^{C=-1}(K^-\pi^+)(K^-\pi^+) = \frac{1}{2} A^4 |1 - R_D e^{-2i\delta}|^2 (x^2 + y^2) \approx \frac{1}{2} A^4 (x^2 + y^2), \tag{29.77}$$

  where $A = |\langle K^-\pi^+ | D^0 \rangle|$ is the real-valued decay amplitudes. This process serves to measure mixing effects.

- $(K^-\pi^+)(K^+\pi^-)$:

$$\Gamma^{C=-1}(K^-\pi^+)(K^+\pi^+) = A^4 \left[1 - 2R_D \cos 2\delta - \frac{1}{2}(x^2 - y^2) \right]. \tag{29.78}$$

  The above process is not sensitive to the mixing measurements since x and y are small, and can be used as a normalization for the previous case.

- $(K^-\pi^+)(S_\chi)$:

$$\Gamma^{C=-1}(K^-\pi^+)(S_\chi) = A^2 A_{S_\chi}^2 |1 + \chi\sqrt{R_D}e^{-i\delta}|^2(1+y^2) \approx A^2 A_{S_\chi}^2(1 + 2\chi\sqrt{R_D}\cos\delta), \tag{29.79}$$

in the SU(3) limit $R_D = \tan^4\theta_C \approx 0.0025$. By comparing rate with $\chi = +1$ final states such as K^+K^- and $\chi = -1$ final states such as K_S (π^0, ω, ϕ), one can measure $\cos\delta$.

- $(K^-\pi^+)(l^-X)$: At $\psi(3770)$ peak, using a leptonic $\overline{D}^0$ flavor tag and defining $A_{l^-} = \langle l^-X|\overline{D}^0\rangle$, one finds [258, 257]

$$\Gamma^{C=-1}(K^-\pi^+)(l^-X) = A^2 A_{l^-}^2 \left[1 - \frac{1}{2}(x^2 - y^2)\right]. \tag{29.80}$$

This process is not sensitive to mixing parameters and serves as a normalization for the next.

- $(K^-\pi^+)(l^+X)$:

$$\Gamma^{C=-1}(K^-\pi^+)(l^+X) = A^2 A_{l^+}^2 \left[R_D + \frac{1}{2}(x^2 - y^2)\right]. \tag{29.81}$$

where $A_{l^+} = \langle l^+X|D^0\rangle = A_{l^-}$. This process is of interesting for mixing parameters if x^2, y^2 R_D are of comparable size but, as mentioned, it is much likely that x^2, $y^2 \ll R_D$ in which case this process can be used to measure R_D.

- $(S_\chi)(l^+X)$:

$$\Gamma^{C=-1}(S_\chi)(l^+X) = A_{S_\chi}^2 A_{l^+}^2(1+y^2). \tag{29.82}$$

The y^2 correction is one order higher than we have been keeping, since $A_{S_\chi}^2$ is already of order $\sqrt{R_D}$. This process serves as a normalization for others.

$C = +1$ $D^0\overline{D}^0$ states:

- $(K^-\pi^+)(K^-\pi^+)$.

$$\Gamma^{C=+1}(K^-\pi^+)(K^-\pi^+) = 4A^4 \left[R_D + \sqrt{R_D}y' + \frac{3}{8}(x^2 + y^2)\right]. \tag{29.83}$$

In this case, the three terms (R_D, y' and R_M) may be measurable. However, most estimates of x and y within the Standard Model are considerably less than a percent [261]. If this is so, the last term in Eq. (29.83) may be inaccessible even through there may exist evidence for the $\sqrt{R_D}y'$ term, and we need an independent determination of δ. This can be obtained in Eq. (29.79).

- $(K^-\pi^+)(K^+\pi^-)$:

$$\Gamma^{C=+1}(K^-\pi^+)(K^+\pi^+) = A^4\left[1 + 2R_D\cos2\delta + 4\sqrt{R_D}(y\cos\delta + x\sin\delta) - \frac{3}{2}(x^2 - y^2)\right] \quad (29.84)$$

  The correction terms are probably unmeasurable, so this process serves as a normalization in comparison w ith previous one.

- $(K^-\pi^+)(S_\chi)$:

$$\Gamma^{C=+1}(K^-\pi^+)(S_\chi) = \approx A^2 A^2_{S_\chi}(1 - 2\chi\sqrt{R_D}\cos\delta)(1 - 2\chi y). \quad (29.85)$$

  This process thus provides information to constrain $\cos\delta$ in case R_D and y are known.

- $(K^-\pi^+)(l^-X)$:

$$\Gamma^{C=+1}(K^-\pi^+)(l^-X) = A^2 A^2_{l^-}\left[1 + 2\sqrt{R_D}(y\cos\delta + x\sin\delta) - \frac{3}{2}(x^2 - y^2)\right] \quad (29.86)$$

- $(K^-\pi^+)(l^+X)$:

$$\Gamma^{C=+1}(K^-\pi^+)(l^+X) = A^2 A^2_{l^+}\left[R_D + 2\sqrt{R_D}y' + \frac{3}{2}(x^2 + y^2)\right]. \quad (29.87)$$

29.3.1 Mixing Rate: R_M

The BESIII experiment at BEPCII searches for $D^0 - \overline{D}^0$ mixing by observing both the hadronic and semileptonic modes of D^0's coming from the decay of the $\psi(3770)$

$$\frac{N(l^\pm l^\pm)}{N(l^\pm l^\mp)} = \frac{x^2 + y^2}{2} = R_M, \quad (29.88)$$

and in hadronic decay modes:

$$\frac{N[(K^-\pi^+)(K^-\pi^+)]}{N[(K^-\pi^+)(K^+\pi^-)]} \approx \frac{x^2 + y^2}{2} = R_M. \quad (29.89)$$

For the case where one final state is hadronic and the other semileptonic, we have

$$\frac{N[(l^+)(K^-\pi^+)]}{N[(l^+)(K^+\pi^-)]} \approx \frac{x^2 + y^2}{2} + R_D, \quad (29.90)$$

where R_D is defined in Eq. (29.33).

The measurement of R_M can be performed unambiguously with the following reactions:

$$\begin{aligned}
&(i)\ e^+e^- \to \psi(3770) \to D^0\overline{D}^0 \to (K^\pm\pi^\mp)(K^\pm\pi^\mp),\\
&(ii)\ e^+e^- \to \psi(3770) \to D^0\overline{D}^0 \to (K^-e^+\nu)(K^-e^+\nu),\\
&(iii) e^+e^- \to D^-D^{*+} \to (K^+\pi^-\pi^-)(\pi^+_{soft}[K^+e^-\nu]),
\end{aligned} \quad (29.91)$$

The observation of reaction (*i*) would be definite evidence for the existence of $D^0-\overline{D}^0$ mixing since the final state $(K^\pm\pi^\mp)(K^\pm\pi^\mp)$ can not be produced from DCS decay due to quantum statistics [227, 245]. In particular, the initial $D^0\overline{D}^0$ pair is in an odd eigenstate of C which will preclude, in the absence of mixing between the D^0 and $\overline{D}^0$ over time, the formation of the symmetric state required by Bose statistics if the decays are to be the same final state. This final state is also very appealing experimentally, because it involves a two-body decay of both charm mesons, with energetic charged particles in the final state that form an overconstrained system. Particle identification is crucial in this measurement because if both the kaon and pion are misidentified in one of the two D-meson decays in the event, it becomes impossible to discern whether mixing has occurred. At BESIII, where the data sample is expected to be 20 fb^{-1} integrated luminosity at $\psi(3770)$ peak, the limit will be $\sqrt{R_M} = 0.4\%$, but only if the particle identification capabilities are adequate. If it were possible to obtain 500 fb^{-1} at the $\psi(3770)$, the limit would be $\sqrt{R_M} = 0.08\%$ [1].

Reactions (*ii*) and (*iii*) offer unambiguous evidence for mixing in that the mixing is searched for in the semileptonic decays for which there are no DCS decay. Of course since the time-evolution is not measured, observation of Reactions (*ii*) and (*iii*) actually would indicate the violation of the selection rule relating the change in charm to the change in leptonic charge which hold true in the standard model [245].

In Table 29.7, the sensitivity for R_M measurements in different decay modes are estimated with 4 years' run at BEPCII.

Table 29.7: *The sensitivity for R_M measurements at BESIII with different decay modes with 4 years' run at BESPCII*

$D^0\overline{D}^0$ Mixing		
Reaction	Events Right Sign	Sensitivity of R_M
$\psi(3770) \to (K^-\pi^+)(K^-\pi^+)$	87195	1×10^{-4}
$\psi(3770) \to (K^-e^+\nu)(K^-e^+\nu)$	94351	
$\psi(3770) \to (K^-e^+\nu)(K^-\mu^+\nu)$	166808	3.7×10^{-4}
$\psi(3770) \to (K^-\mu^+\nu)(K^-\mu^+\nu)$	83404	
$D^{*+}D^- \to [\pi_s^+(K^+e^-\overline{\nu})(K^+\pi^-\pi^-)]$	76000	
$D^{*+}D^- \to [\pi_s^+(K^+\mu^-\overline{\nu})(K^+\pi^-\pi^-)]$	60000	
$D^{*+}D^- \to [\pi_s^+(K^+e^-\overline{\nu})$(other D^- tag)]	60000	4.7×10^{-5}
$D^{*+}D^- \to [\pi_s^+(K^+\mu^-\overline{\nu})$(other D^- tag)]	60000	

29.3.2 Doubly Cabibbo Suppressed Rate and Strong Phase $\cos\delta_{K\pi}$

Doubly Cabibbo suppressed (DCS) decays of the D^0 mesons, and D^0 mixing, give rise to identical final states. The two processes can only be distinguished by their different time dependance, or at the $\psi(3770)$ peak, by taking advantage of effects due to quantum statistics as discussed in Section 29.3.1. In Eq. 29.45 of Section 29.2.2, the wrong-sign

decay rate relative to the right-sign rate is defined as

$$R_{WS} = R_D + \sqrt{R_D}y' + \frac{1}{2}R_M\,, \tag{29.92}$$

in absence of mixing, $R_{WS} = R_D = |A_f/\overline{A}_f|^2$. In general, the ratio of DCS decay rate relative to CF decay rate is $R_D \sim \tan^4\theta_C \sim 0.25\%$, where θ_C is the Cabibbo angle. However, as pointed out in Ref. [227], $\tan^4\theta_C$ is not the only suppression factor, the ratio may be various for different final state, such as $R_D \sim 2.1 \times \tan^4\theta_C$ for $D^0 \to K^+\pi^-$, while $R_D \sim 0.45 \times \tan^4\theta_C$ for $D^0 \to K^+\rho^-$ due to final state interaction [227].

One can also measure R_D in the multibody channels $D^0 \to K^+\pi^-\pi^0$ and $D^0 \to K^+\pi^-\pi^+\pi^+$ as discussed in Section 29.2.2.

At BESIII, at $\psi(3770)$ peak, the semileptonic decay can be used to tag hadronic decay on the other side, as the case in Eq. 29.90, by neglecting mixing effect, one got [258]

$$\frac{N[(l^+)(K^-\pi^+)]}{N[(l^+)(K^+\pi^-)]} \sim R_D, \tag{29.93}$$

since it is much more likely that x^2, $y^2 \ll R_D$, this processes can be used to measure R_D directly.

We can also take advantage of the coherence of the D^0 mesons produced at the $\psi(3770)$ peak to extract the strong phase difference δ between DCS and CF decay amplitudes that appears in the time-dependent mixing measurement in Eq. 29.44. Because the CP properties of the final states produced in the decay of the $\psi(3770)$ are anti-correlated, one D^0 state decaying into a final state with definite CP properties immediately identified or tags the CP properties of the other side. As discussed in Ref. [258], from Eq. 29.70, the process of one D^0 decaying to $K^-\pi^+$, while another D^0 decaying to a CP eigenstate S_χ with eigenvalue $\chi = \pm 1$ can be described as

$$\Gamma(K^-\pi^+, S_\chi) = A^2 A_{S_\chi}^2 |1 + \chi\sqrt{R_D}e^{-i\delta}|^2(1+y^2) \approx A^2 A_{S_\chi}^2(1 + 2\chi\sqrt{R_D}\cos\delta), \tag{29.94}$$

where $A = |\langle K^-\pi^+|D^0\rangle|$ and $A_{S_\chi} = |\langle S_\chi|D^0\rangle|$ are the real-valued decay amplitudes. In order to estimate the total sample of events needed to perform a useful measurement of δ, we define [258] an asymmetry

$$\mathcal{A} \equiv \frac{\Gamma(S_+) - \Gamma(S_-)}{\Gamma(S_+) - \Gamma(S_-)}, \tag{29.95}$$

where $\Gamma(S_\pm)$ is a rate for the $\psi(3770) \to D^0\overline{D}^0$ configuration to decay into a flavor eigenstate and a CP-eigenstate $S_\pm$. Eq. 29.94 implies a small asymmetry, $\mathcal{A} = 2\sqrt{R_D}\cos\delta$. For a small asymmetry, a general result is that its error $\Delta\mathcal{A}$ is approximately $1/\sqrt{N}$, where N is the total number of events tagged with CP-even and CP-odd eigenstates. Thus we have

$$\Delta(\cos\delta) \approx \frac{1}{2\sqrt{R_D}\sqrt{N}}. \tag{29.96}$$

The number N of CP-tagged events decaying to $K^-\pi^+$ is related to the total number of $D^0\overline{D}^0$ pairs $N(D^0\overline{D}^0)$ through $N \approx N(D^0\overline{D}^0)\mathcal{BR}(D^0 \to K^-\pi^+) \times \mathcal{BR}(D^0 \to S_\pm) \times$

$\epsilon_{tag} \approx 4.0 \times 10^{-4} N(D^0\overline{D}^0)$, here we assume the branching ratio-times-efficiency factor ($\mathcal{BR}(D^0 \to S_\pm) \times \epsilon_{tag}$) for tagging CP eigenstates is about 1.1% (the total branching ratio into CP eigenstates is larger than about 5% [90]). With the estimation of $R_D = 1.4 \times \tan^4\theta_C \approx 0.3\%$, one found [258]

$$\Delta(\cos\delta) \approx \frac{400}{\sqrt{N(D^0\overline{D}^0)}}. \tag{29.97}$$

At BESIII, about 72×10^6 $D^0\overline{D}^0$ pairs can be collected with 4 years' run. We are entitled to a factor of 2 for considering both $K^-\pi^+$ and $K^+\pi-$ final states. We thus estimate that one may be able to reach an accuracy of about 0.05 in $\cos\delta$.

29.3.3 The Comprehensive Quantum Correlation Analysis